10

Mechanical Properties of Fine-Grained Magnesium Alloys Processed by Severe Plastic Forging

Taku Sakai and Hiromi Miura
UEC Tokyo (The University of Electro-Communications)
Japan

1. Introduction

Magnesium (Mg) and its alloys have recently attracted growing interest especially in the automobile industries due to their excellent specific properties, as one of the lightest structural materials (Mordike & Ebert, 2001). To date, most of Mg products have been fabricated by casting, in particular, by die-casting because of its high productivity, suitable strength, acceptable quality and dimensional accuracy. The intrinsic poor formability and limited ductility at ambient temperature due to the hexagonal close-packed (hcp) crystal structure and the associated insufficient independent slip systems, however, greatly restricts their practical usage. Then Mg and its alloys are categorized in hard plastic materials and its products of structural light materials are not a lot fabricated by plastic working such as rolling, forging and other forming processes. During warm and hot working, on the other hand, there are several non-basal slip systems operated in addition to the basal slip plane leading to increase of the plastic workability. It is also known that fine-grained structures are frequently developed in Mg alloys after warm and hot working to relatively low strains. The plastic workability of such fine-grained alloys can be much improved accompanied by superplasticity. It has been studied recently (Humphrey & Hatherly, 2004, Valiev & Langdon, 2006) that severe plastic deformation (SPD), such as equal channel angular pressing (ECAP), high pressure torsion (HPT), accumulative roll-bonding, multi-directional forging (MDF), etc., is carried out on many metallic materials, leading to the development of ultrafine-grained (UFGed) structures in a whole volume of the products. The present authors have studied thermomechanical processing for development of UFGed Mg alloys by using MDF under decreasing temperature conditions, and succeeded much in improvement of the plastic workability as well as the mechanical properties at ambient temperature, as described in the following sections.

The aim of the present chapter is to review our current studies on (1) the mechanical and microstructural behaviors as well as the grain refinement mechanism operating in Mg alloys during a single-pass compression, (2) outstanding effect of MDF on acceleration of rapid grain refinement under decreasing temperature conditions, and (3) improvement of the mechanical properties of fine-grained Mg alloys processed by MDF. The mechanical properties and characteristics of superplasticity are investigated in tension at various temperatures and strain rates, and the microstructural and textural changes taking place

during tensile deformation are examined. The mechanisms of new grain development taking place during plastic working and the deformation mechanisms operating in fine-grained Mg alloys are discussed in details.

2. Experimental procedure

2.1 Materials and thermomechanical procedure

Commercial Mg alloys, such as AZ31, AZ61, etc., were provided as hot-extruded rods. Cylindrical samples of 8 mm in diameter and 12 mm in height were prepared from the rod with the axis aligned along the extrusion (longitudinal) direction and mainly used for studying the deformation behaviors during a single-pass compression. Another type of samples was a rectangular shape with the dimensions of the axis ratio of 2.22: 1.49: 1 and used for studying the deformation behaviors and the processes of grain refinement taking place during MDF. The MDF employed is carried out with changing the loading axis at an angle of 90° through three mutually perpendicular axes (i.e. x to y to z to x to …..) from pass to pass (Fig. 1). When a pass strain is kept as $\Delta\varepsilon = 0.8$, the dimension ratio above mentioned does not change in each compression and so MDF can be carried out repeatedly to severe large accumulated strains. Then these samples machined were annealed at 733 K for 7.2 ks and furnace cooled, leading to the evolution of almost equiaxed grains with a diameter of about 22.3 μm (see Fig. 4(a)).

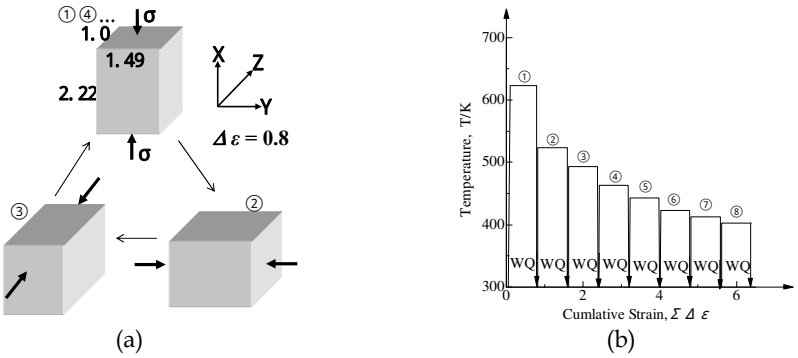

Fig. 1. Schematic illustration of the thermo-mechanical processing used in MDF with continuous decreasing temperature in each pass. (a) The loading direction is changed in 90° with pass to pass (x→y→z→x···). A pass strain $\Delta\varepsilon$ is 0.8. (b) Deformation temperature is decreased from 623K to 423K in each MDF. WQ indicates water quenching.

Multiple forgings were carried out in compression by using the rectangular samples with a dimension of 31 mm in length, 21 mm in width and 14 mm in thickness or with the other dimension of around 60 x 40 x 27 mm^3, which were machined from the as-extruded rod parallel to the extrusion direction. Compression were carried out at constant true strain rates in a modified Instron-type testing machine which was equipped both a vacuum vessel and a quenching apparatus (Sakai & Takahashi, 1991). The later made a sample possible to quench in water within 1 s after hot deformation was ceased for freezing the as-deformed microstructures. The samples were deformed either isothermally in single-pass compression or in repeated MDF at various temperatures between 473 K and 673 K. MDF was also

performed under decreasing temperature conditions pass by pass from 623 K to 403 K because of promotion of rapid grain refinement (Fig. 1). The samples MDFed were cut along a plane parallel to the last compression axis for microstructural observation, which was carried out by using optical microscopy (OM), transmission electron microscopy (TEM) under an accelerating voltage of 200 kV and scanning electron microscopy (SEM) in corporating an orientation imaging microscopy (OIM) system

2.2 Tensile test

A strong texture was developed with the basal plane, i.e. {0001}, roughly perpendicular to final forging direction in the fine-grained Mg alloy, which is typical for compressed hcp-metals (see Fig. 7) (Rollet & Wright, 1998). Three perpendicular directions of the Mg samples MDFed were defined as L (=X), LT (=Y) and ST (=Z), respectively, as shown in Figs. 1 and 2. Two types of tensile specimens were machined from the Mg plate MDFed for studying mainly (1) the mechanical properties at room and elevated temperatures, and partly (2) influence of the texture anisotropy on the properties. For tensile tests of the formers (1), the specimens with the gauge dimension of 6 mm in length, 3 mm in width, and 0.7 mm in thickness were machined from the Mg plate parallel to the L-ST plane. These correspond to the 0° specimen in Fig. 2(b). For tensile tests of the latters (2), three kinds of tensile specimens with a gauge dimension of 10 × 4 × 1 mm^3 were machined from the Mg products MDFed, as shown schematically in Fig. 2(b). The tensile axes for each specimen were inclined at 0°, 45° and 90° to the basal plane, respectively. Hereafter these specimens are denoted as the 0°, 45° and 90° ones.

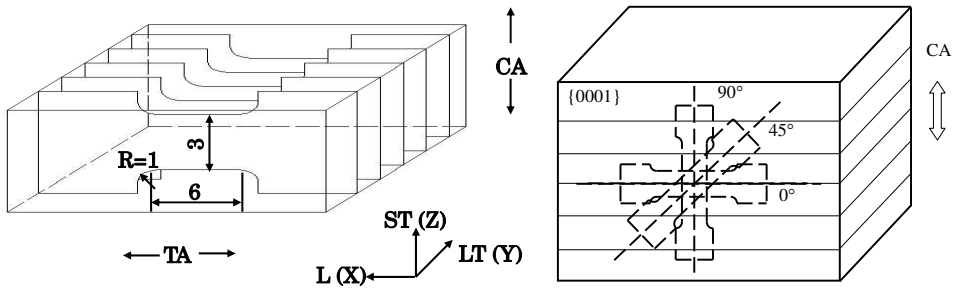

(a) (b)

Fig. 2. (a) Tensile specimens, machined parallel to L-ST plane of MDFed Mg alloy, for studying mechanical properties and superplasticity of fine-grained Mg alloy. These correspond to the 0° ones in (b). (b) Tensile specimens for studying effect of the texture anisotropy of MDFed Mg alloy on mechanical behaviors. Tensile axes are inclined at 0°, 45° and 90° to the basal plane, which is roughly perpendicular to final compression axis (CA).

Tensile tests were conducted in vacuum by using an Instron-type testing machine, which was equipped with a hydrogen gas quenching apparatus (Xing et al., 2007). Tensile tests were carried out at temperatures from 298 K to 473 K and at initial strain rates from around 10^{-6} s^{-1} to 10^{-2} s^{-1}. The specimens were heated and kept for 0.6 ks at each test temperature, and then tensile tested, followed by rapid cooling at a rate of around 0.5 Ks^{-1} for freezing as-deformed microstructures. The microstructures were examined by using OM and OIM. The texture changes were also examined.

3. Mechanical and microstructural behaviors during hot compression

A series of the true stress-true strain (σ–ε) curves in compression at a true strain rate of 3×10^{-3} s^{-1} for an annealed Mg alloy AZ31 is represented in Fig. 3 (Yang et al., 2003). At high temperatures above 573 K, the σ–ε curves show work softening following a smooth stress peak at low strain, followed by steady-state like flow at high strains. Such flow behaviors are generally similar to those of conventional discontinuous dynamic recrystallization (dDRX) behavior appearing in cubic metals, where new grains with high angle boundaries (HABs) are dynamically nucleated and then followed by their growth in large distance, that is two-step reactions (Sakai & Jonas, 1984, 2001). At low temperatures below 523 K, in contrast, the σ–ε curve shows rapid work hardening in low strain and a sharp stress peak at around ε = 0.2, and then work softening followed by steady state flow at high strains. The σ–ε curve at 473 K exhibits a sharp and higher stress peak of above 300 MPa at around ε = 0.2, immediately followed by brittle fracture.

Typical microstructural changes and the corresponding σ - ε curve for the Mg alloy deformed at 673 K and at 3 x 10^{-3} s^{-1} are shown in Fig. 4 (Yang et al., 2003). The relatively smooth grain boundaries of the initial structure (Fig. 4(a)) are frequently corrugated and fine grains are partly evolved near the boundaries at around the peak strain ε_p = 0.12 where the stress peak appears (Fig. 4(b)). It was observed from the surface morphology that several deformation bands based on **kink bands** (Higashida et al., 1986) are frequently evolved and traversed or intersected in some grain interiors. The boundaries of these bands can be seen in the OIM map in Fig. 5(a). At a strain of 0.3, where strain softening clearly takes place, new fine grains are developed in colony along most the grain boundaries accompanied with grain boundary sliding and grain rotation (Fig. 4(c)). Further straining to around 0.5, where a steady state flow starts to take place, there are equiaxed new grains developed homogeneously and almost fully in the whole area (Fig. 4(d)). The results in Fig. 4 are almost similar to the previous ones reported by Ion et al., 1982 and Sitdikov & Kaibyshev, 2001. The close relationship between the flow softening behavior and the development of a new grain structure looks like the same as that of conventional dDRX in cubic metals (Sakai & Jonas, 1984, 2001).

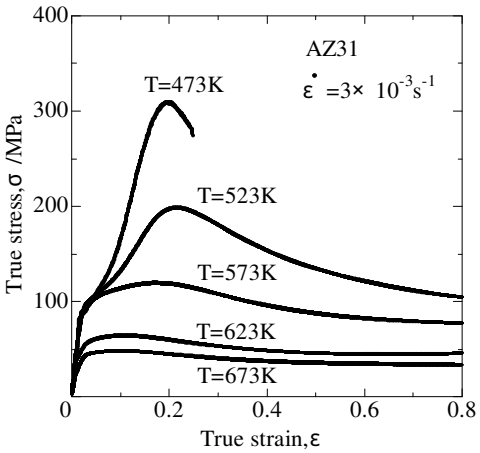

Fig. 3. Temperature effect on true stress-true strain curves of as-annealed AZ31 alloy with a grain size of 22.3 μm during single pass compression at a true strain rate of 3×10^{-3} s^{-1}.

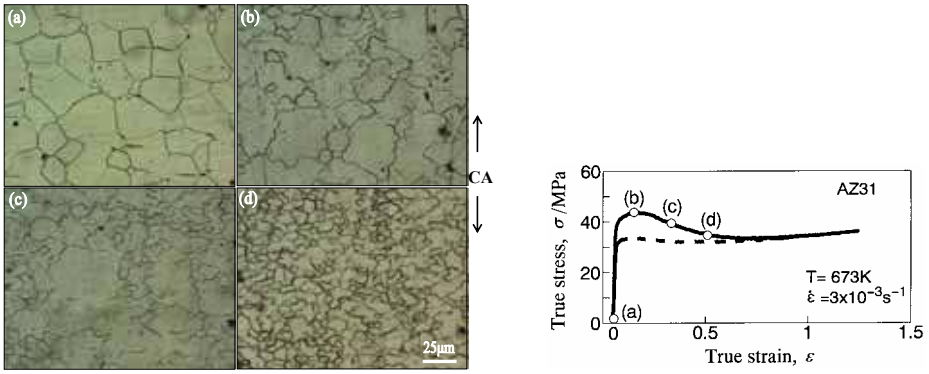

Fig. 4. Typical optical microstructures and the corresponding true stress-true strain curve of AZ31 alloy deformed to various strains at 673 K and at 3 x 10 $^{-3}$s^{-1}, followed by water quenching. The compression axis (CA) was parallel to the extrusion direction of the alloy. (a) $\varepsilon = 0$, (b) $\varepsilon = 0.1$, (c) $\varepsilon = 0.3$ and (d) $\varepsilon = 0.5$.

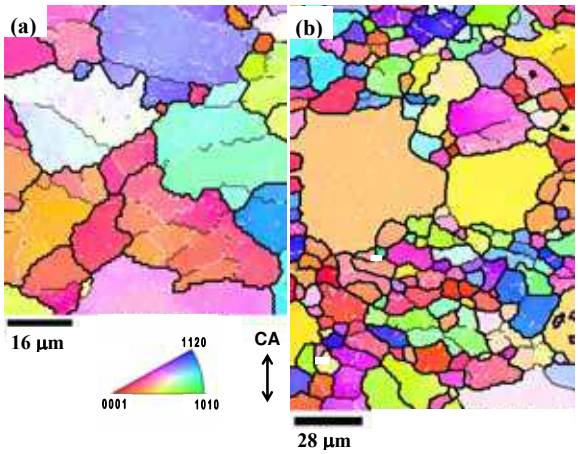

Fig. 5. Typical OIM maps of AZ31 alloy deformed to strains of (a) 0.10 and (b) 0.30 at 673 K and at 3 x 10 $^{-3}$ s $^{-1}$.

Typical OIM micrographs for the sample deformed to strains of 0.1 and 0.3 at 673 K are shown in Fig. 5 (Yang et al., 2003). Different colors for each grain and even in grain interiors indicate different crystallographic orientations defined in the inverse pole figure. HABs with misorientations more than 15° are delineated by thick-black lines, while low-angle boundaries in the range of 4° and 15° by thin-black lines and those in the range 2°- 4° by white lines. It is seen in Fig. 5(a) that fine grains are partly evolved along grain boundaries corrugated, and new boundaries with medium angle misorientations are developed in some regions of corrugated boundaries. Such a process of new grain formation may be similar to that appearing in conventional dDRX in cubic metals, i.e. the bulging of part of serrated grain boundaries (Sakai & Jonas, 1984, 2001). New boundaries with low to medium angle misorientations are also evolved in some grain interiors and some of them intersect with

each other. These new boundaries with low misorientation angles correspond to those of kink bands and so similar to transition bands or microbands (Humphreys & Hatherly, 2004). It is interesting to note in Fig. 5(a) that several initial grains are fragmented by the formation of such kink bands and the crystal orientation of each region fragmented is slightly changed in a grain interior even at $\varepsilon = 0.1$.

A typical OIM micrograph for a strain of 0.3 is depicted in Fig. 5(b). In the strain range over around ε_p, where a work softening takes place, the fraction of new grains rapidly increases and finally an equiaxed new grain structure is homogeneously developed in $\varepsilon > 0.5$ throughout the material. It is seen in Fig. 5 (b) that crystal orientation of each new grain evolved are almost randomly distributed and some rather coarser grains are retained in the fine grained regions. It is noted here that small angle subboundaries related to kink bands are not developed in these retained grain interiors. It was remarkable to note that the average size of new grains evolved is roughly similar to that of the regions fragmented by kink band and also does not change during further deformation to high strains. This suggests that each fragmented region surrounded by low to medium angle boundaries may transform in-situ to a grain with HABs and also scarcely grow during further deformation.

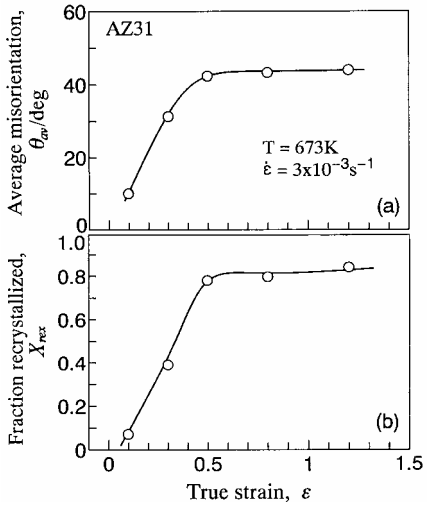

Fig. 6. Strain dependence of (a) average misorientation of (sub)grain boundaries, θ_{av}, and (b) fraction dynamically recrystallized, X_{rex}, of AZ31 alloy deformed at 673 K and at 3 x $10^{-3}s^{-1}$.

Changes, with increasing deformation, of the average misorientation (θ_{av}) and of the volume fraction of a new grain structure (X_{rex}) measured in OIM maps are depicted in Fig. 6 (Yang et al., 2003). Both the θ_{av} and X_{rex} start to increase at around the peak strain and rapidly rise during work softening, finally approaching saturation values at high strains, i.e. about 43°and 0.85, respectively. It is interesting to note in Fig. 6(b) that new grains are not fully developed even under a steady state flow in high strain. Such a result has not been reported in conventional dDRX of cubic metals. All of the results mentioned above suggest that new grain evolution in the Mg alloy may be not resulted from conventional dDRX, but a series of strain-induced reactions, that is essentially similar to **continuous DRX (cDRX)**. This will be discussed in section 4 in detail.

Finally, let us discuss a possible relationship between work softening after the peak stress and texture change occurring during compression. The extruded Mg rod with a strong texture, as mentioned above, is confirmed by the results of Fig**. 7** (Yang et al., 2002, 2003). Here the L-direction sample at $\varepsilon = 0$ has the basal plane of hcp lattice lying parallel to the extrusion direction and so the compression direction. According to the method employed by Ion et al. (1982), relative intensity of the texture orientations measured in the OIM data is plotted against φ, the angle between the compression axis and the {0001} texture. It is seen in Fig. 7 that the initial texture of the L-direction sample is reoriented gradually by compression. Namely, the alignment of the basal planes initially parallel to the compression axis is gradually rotated by compression and approaches perpendicular to the compression axis in high strain. The initial texture of the T-direction sample, prepared from the extruded rod aligned along the transverse direction, in contrast, was scarcely changed by compression and the relative intensity increased with increasing strain. It is quite possible to note, therefore, that work softening taking peace only in the L-direction sample can not result from new grain development due to DRX, but also the initial texture in which slip hardly takes place changing to the softer or stable one, that is the **geometrical softening**. It is also well understood why an appreciable work softening does not take place in the T-direction sample because of no clear change in the texture.

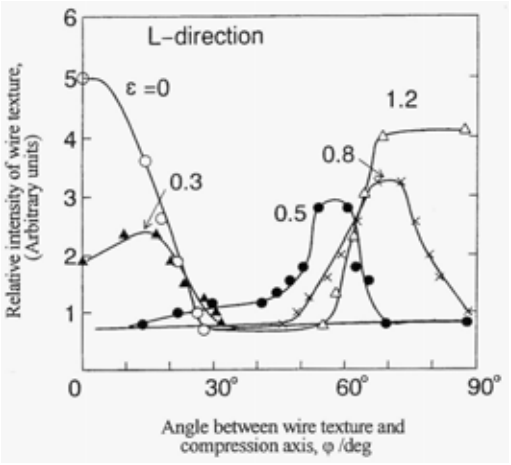

Fig. 7. Changes in the distribution of wire texture, with the basal planes lying parallel to the extruded direction, with compression at 673K. The axes of the L- direction samples is parallel to the extrusion direction.

4. Mechanisms of grain refinement in Mg alloy

It is seen from the experimental results and discussion in section 3 that hot deformation behavior of the Mg alloy AZ31 is closely related to the new grain formation due to the operation of DRX. Some results are, however, not similar to those of conventional dDRX taking place in cubic metals, although some previous studies on Mg alloys discuss that dDRX takes place during hot deformation (Ion et al., 1982, Sitdikov & Kaibyshev., 2001, Miura et al., 2005). So let us summarize briefly new grain formation due to dDRX taking

place in cubic metals during hot deformation. It is well known (Sakai & Jonas, 1984, 2001) that new grains are mostly evolved along the initial grain boundaries which are serrated by preceding hot deformation, and DRX nucleation occurs by operation of the bulge mechanism of the following process. Grain boundary sliding and/or grain boundary zone shearing first operates at appropriate serrated boundaries, leading to development of inhomogeneous local strains as well as strain or orientation gradients developed from grain boundaries towards grain interiors (Miura et al., 1994, 2007, Belyakov et al., 1998, Wusatowska-Sarnek et al., 2002). With further deformation, dislocation boundary and/or twin boundary is easily evolved in near the extrapolated places of the prior grain boundaries, resulting in acceleration of the separation of the bulged region from the parent grains and then dynamic formation of new grains. Finally these new grains can grow towards grain interiors because of large gradients of strain energy developed, finally leading to a full development of new grains in a whole volume.

The mechanisms of DRX nucleation taking place in Mg alloy will be discussed now. During early hot deformation of Mg alloy, kink bands are frequently formed in the regions of corrugated grain boundaries and also crossed in grain interiors. Then the misorientation and the number of the boundaries of kink band rapidly rise with further deformation (Fig.6). Then the regions fragmented by kink bands are bounded by HABs, but do not grow with further deformation. These regions finally result in evolution in-situ of new grains assisted by dynamic recovery. It is concluded, therefore, that the dynamic formation of new grains discussed above can result from a series of strain-induced continuous reactions, that is essentially similar to cDRX and actually a one-step phenomenon, i.e. new grains are nucleated homogeneously throughout the material and can scarcely grow (Sakai & Jonas, 2001). In contrast, conventional dDRX involves a two-step process, i.e. the nucleation of new grain surrounded by HABs followed by their long distance migration. It should be noted in cDRX of Mg alloy that a new grain structure can not be fully developed throughout the material even in high strain (Fig. 6). In retained original grains surrounded by new fine grains, kink bands may be hardly developed, because constrained deformation by surrounding grains can be relaxed by grain boundary sliding and dynamic recovery, etc., which take frequently place in the fine grained regions during deformation.

It has been recently reported, by the way, that UFGs are developed in many cubic metallic materials by **severe plastic deformation (SPD)**, such as ECAP, HPT, MDF, etc., and considered to be resulted from strain-induced continuous reactions, i.e. cDRX (Belyakov et al., 2001, Humphreys & Hatherly, 2004, Sakai et al., 2008). So let us discuss the process of strain-induced grain formation in Mg alloy as well as in cubic metals during SPD. The continuous increase in misorientations between (sub)grain boundaries evolved during deformation is an essential feature of cDRX, and the kinetics can be discussed by using the relationship between the average (sub)grain boundary misorientation (θ_{AV}) and total accumulated strain (Sakai et al., 2008). The θ_{AV} – ε relationships for Al alloy 2219 ECAPed at 523 K (Mazurina et al., 2008), a pure Cu MDFed at 195 K to 473 K (Gao et al., 1999, Belyakov et al., 2001, Kobayashi et al., 2007) and Mg alloy AZ31 compressed at 673 K are represented in Fig. 8. The data of AZ31 is the same as those in Fig. 6. It is remarkable to note in Fig. 8 that the kinetics of grain formation clearly depends on materials and is highest in the Mg alloy AZ31. The process of misorientation increase can be virtually subdivided into three stages in Fig. 8. The first stage is characterized by a rapid rise in θ_{AV} followed by a small plateau at a level of about 5°. Then the misorientation starts to increase again rapidly after some critical strain ε_c, i.e. this is in the second stage. The third stage corresponding to large strains, the

θ_{AV} approaches its saturation level. The fraction of HABs vs. strain (F_{HAB} – ε) curves are also similar to those in the θ_{AV} – ε curves in Fig. 8 (Sakai et al., 2008). The F_{HAB} is scarcely developed at below ε_c (the first stage) and then the F_{HAB} starts to increase in the second stage and approaches a saturation value in high strain (the third stage). It is also clearly seen in Fig. 8 that temperature effect on the kinetics of grain refinement in Cu is negligible small in the first and second stages of the evolutional process. However, the kinetics of new grain formation in the third stage slows down with decrease of deformation temperature. As a result, the saturation level of θ_{AV} at large strains is remarkably lower for deformation at lower temperature.

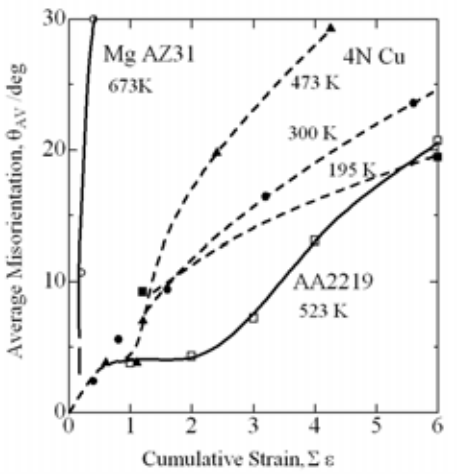

Fig. 8. Relationships between average misorientation angle of strain-induced (sub)grain boundaries and cumulative strain of Al alloy 2219 ECAPed at 523 K, pure Cu MDFed at 195 K, 300 K and 473 K, and Mg alloy AZ31 compressed at 673 K.

Now let us discuss the mechanisms for strain-induced grain formation operating in cubic metals during SPD and also in Mg alloy during light deformation, respectively. The structural changes leading to the submicrocrystalline structure after large strains by SPD of cubic metals can be illustrated by a schematic drawing in Fig. 9 (Sakai et al., 2008). In the first stage of the process, i.e. $0 < \varepsilon < \varepsilon_c$, early deformation brings about high density dislocations that are homogeneously arranged in cellular substructure. The initiation of rapid increase in θ_{AV} over ε_c can be resulted from the introduction of deformation bands such as **microshear bands** (**MSBs**) in cubic metals, followed by the fragmentation of original grains in the second stage of the process. The crystal orientation of small adjacent domains separated by a sharp MSB, *e.g.* the domains labeled with A and B in Fig. 9(a), seems to be the same at around ε_c. The new fine grains are preferably evolved inside the MSBs and, especially, at their intersections (Fig. 9(b)). The fraction of the UFGed structure gradually increases with increasing the number of MSB. It can be concluded, therefore, that a full evolution of new fine grains in cubic metals must need a full development of MSB in a whole volume that is promoted by further SPD. In Mg alloys, on the other hand, kink bands in replacement of MSB are frequently developed in grain interiors after hot deformation to much low strains and these fragmented regions can become in-situ new grains with HABs

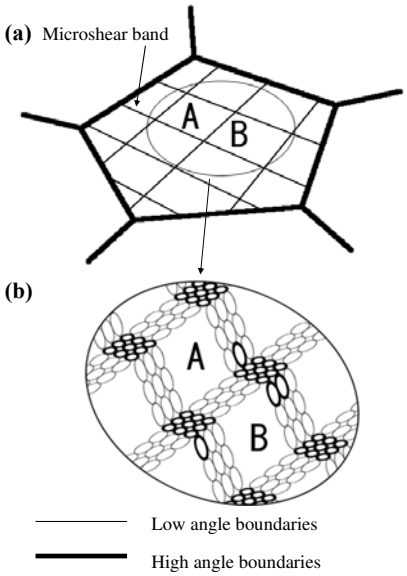

Fig. 9. Schematic drawing of the development of (a) microsher bands at low strains and (b) subsequent formation of new grains at the intersections and along the microshear bands at large strains in cubic metals.

in low strain (Fig. 8). This means that kink bands do not need to be fully evolved in high density in a whole volume of Mg alloys. If MSBs are changed to kink bands in the model of Fig. 9(a), new grains can be fully developed in a whole volume even after light deformation, because grain formation can result from grain fragmentation due to introduction of kink bands in the case of Mg alloy.

5. Effect of MDF on grain refinement

It is discussed in section 4 that dynamic grain refinement taking place in Mg alloy during hot deformation can be based on grain fragmentation due to kink band evolving in original grain interiors and so controlled by strain-induced continuous reactions assisted by dynamic recovery, i.e. cDRX. The new grain development starts to take place at low strains and rapidly approach a saturation state at strains over $\varepsilon > 0.5 - 0.6$ (Figs. 4 and 6). At the same time, the basal plane roughly parallel to the compression axis in extruded Mg rod gradually rotates and approaches perpendicular to the compression axis at around $\varepsilon > 1$ (Fig. 7). On the other hand, kink bands are concurrently formed roughly perpendicular to the basal plane in low strain (Yang et al, 2006) and so new fine grains may not be fully generated throughout the material during a single-pass compression (Fig. 6). Aiming to break this difficulty, any effect of the change of the loading direction on further grain refinement has been studied systematically by using the same Mg alloy AZ31. It has been also known in Mg alloys that dynamic grain sizes evolved in high strain decrease with decreasing deformation temperature (Galiyev et al. 2001, Sitdikov & Kaibyshev 2001). Then if Mg alloy is repeatedly MDFed with decreasing temperature, grain refinement is expected to take place more rapidly and effectively.

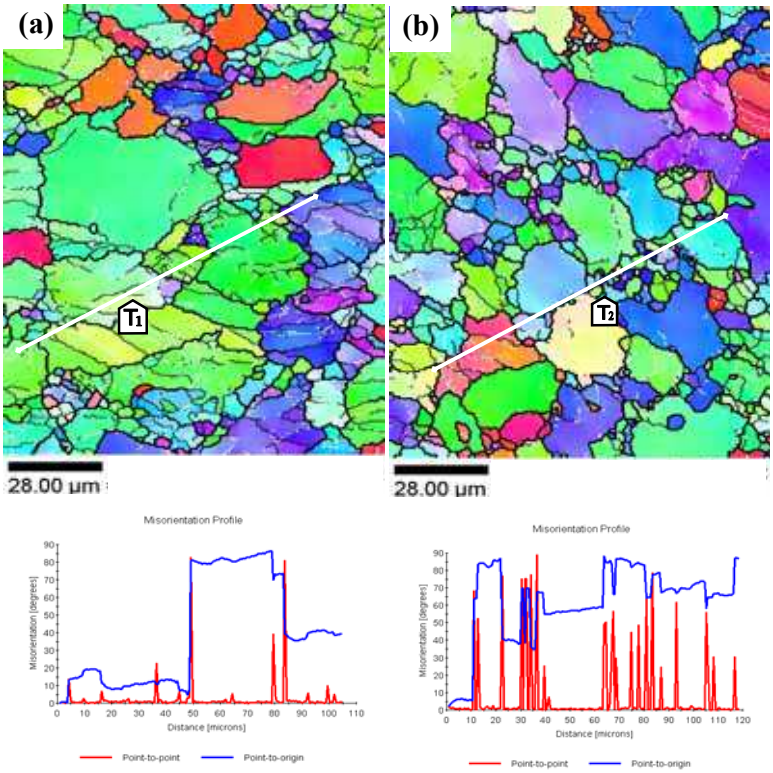

Fig. 10. OIM maps of Mg alloy AZ31 deformed to ε= 0.3 at 573 K by (a) a single- and (b) two-directional compression with changing the loading direction. Point-to-point misorientations and lattice rotation measured along the lines T_1 and T_2.

A typical effect of MDF on grain evolution can be seen in Fig. 10 (Yang et al., 2007), where two typical OIM micrographs show the microstructures developed during single- and two-directional compression at a lower temperature of 573 K. The former sample was compressed once to $\varepsilon = 0.3$ and the latter one deformed twice to $\Delta\varepsilon = 0.15$ in each direction, resulting in a same total strain, i.e. $\Sigma\ \Delta\varepsilon = 0.3$. The distribution of point-to-point misorientation (θ) and cumulative disorientation ($\Sigma\theta$) developed along the lines T_1 and T_2 are also represented in Fig. 10. Under a single-directional compression, kink bands developed mainly in one direction, which are roughly perpendicular to the compression axis (Fig. 10 (a)). Misorientation angle of deformation-induced boundaries does not exceed 20° in original grain interiors after a single-directional compression. Under two-directional compression with changing the loading direction, in contrast, the development of kink bands and their intersection as well as new grains takes place more frequently at a same total strain (Fig. 10 (b)). It is remarkable to note that kink bands are developed in various directions accompanied by changing the loading direction, leading to rapid formation of new grain boundaries with misorientations of over 20°. Such results in Fig. 10 strongly suggest that MDF may be a more effective method on strain-induced grain refinement taking place in Mg alloys. It can be seen in Fig. 10 that, in addition to the above mechanisms,

mechanical twinning may effectively contribute to the grain fragmentation in coarse grains, in particular, under decreasing temperature conditions (Sitdikov et al., 2003, Miura et al., 2007, Yang et al., 2007).

Let us discuss the process of grain refinement taking place in the Mg alloy during MDF under dropping temperature condition. MDF with a pass strain of 0.8 was carried out on the same Mg alloy AZ31 with decreasing temperature from 623 K to 403 K from pass to pass. Fig. 11 shows typical true stress-cumulative strain ($\sigma - \Sigma\Delta\varepsilon$) curves during repeated MDF under decreasing temperature condition and also during isothermal MDF at 623 K (Xing et al., 2008). The first flow curve at 623 K shows a sharp stress peak followed by work softening and subsequently steady-state like flow at high strains. The amounts of the peak stress and work softening after the peak decrease with repeated isothermal MDF at 623 K (broken line), while the flow stresses of around 40 MPa appearing in high cumulative strain do not change during MDF. On the other hand, the σ–$\Sigma\Delta\varepsilon$ curves during MDF with decreasing temperature condition are depicted by solid line in Fig. 11. During early MDF at higher temperatures, they show work softening following a peak stress and then followed by steady-state flow. With dropping the processing temperature, the values of flow stress increase accompanying with decrease in the amount of work softening after the stress peak. At temperatures below 493 K, steady-state flow appears without a peak stress as well as flow softening. It is interesting to note that the $\sigma - \varepsilon$ curve for the as-annealed sample at 473 K (see Fig. 3) and that appearing at around $\sum\Delta\varepsilon$ =3 during MDF at 473 K in Fig. 11 is clearly different from each other. Namely, the flow stress peak for the annealed sample is 310 MPa a ε =0.2 and then brittle fracture occures (Fig. 3) and, in contrast, that appearing during MDF at 473 K is about 128 MPa which is about one-third of the former. Furthermore, the MDF processing is successful to deform the Mg alloy to cumulative large strains up to $\sum\Delta\varepsilon$ =5.6 at 403 K which is below than $0.5T_m$ (T_m is the melting point).

Typical grain structural changes taking place during MDF under decreasing temperature condition is represented in Fig. 12 (Xing et al., 2008). It is seen in Fig. 12 that strain-induced grain sizes developed decrease sensitively with decreasing temperature from 623 K to 403 K

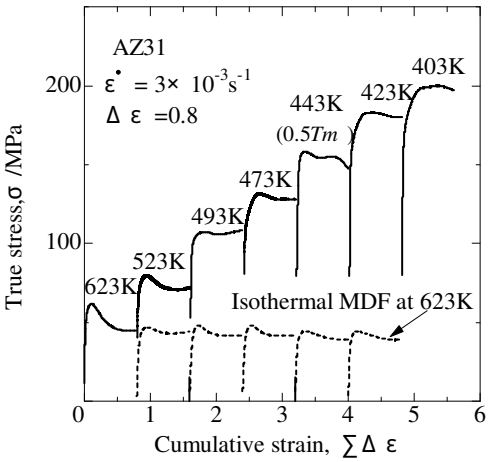

Fig. 11. True stress-true strain curves of AZ31 alloy during isothermal MDF at 623K (broken line) and MDF under decreasing temperature condition from 623K to 403K (solid line).

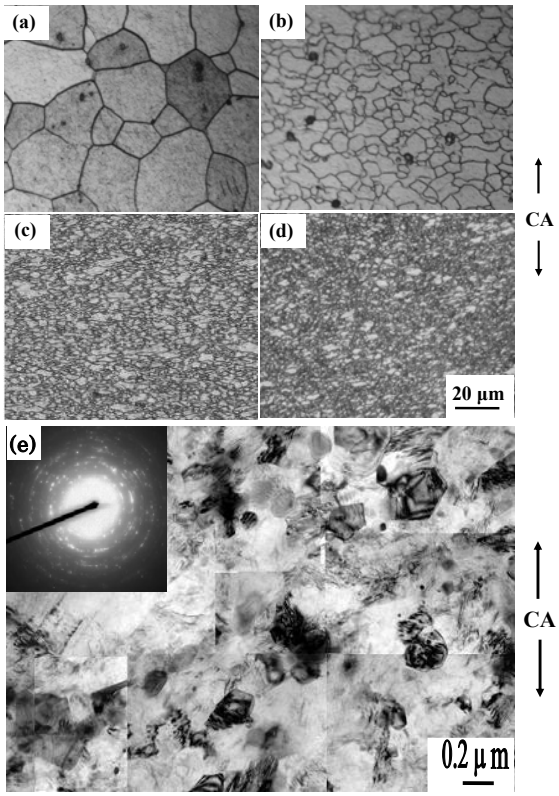

Fig. 12. Optical ((a) to (d)) and TEM (e) microstructures with the diffraction pattern evolved in Mg alloy AZ31 during MDF with continuous decreasing temperature in each pass. (a) As annealed, (b) T = 623 K, $\Sigma\Delta\varepsilon$ = 0.8, (c) T = 523 K, $\Sigma\Delta\varepsilon$ =1.6, (d) T = 473K, $\Sigma\Delta\varepsilon$ =3.2, and (e) T = 403K, $\Sigma\Delta\varepsilon$ =5.6.

during MDF. Fig. 12 (e) shows a typical TEM microstructure and the selected area diffraction (SAD) pattern developed in the sample deformed to $\Sigma\Delta\varepsilon$ = 5.6 at 403 K. Many diffraction points with a streak in the SAD pattern suggest that rather large internal stresses can be evolved in this strain-induced grain structure (Belyakov et al., 2000). The SAD pattern in Fig. 12 (e), showing almost uniform and fully continuous rings, suggests that this microstructure is composed of polycrystalline UFGs surrounded by HABs. The average grain size of 0.23 μm is almost fully developed after 7th-pass compression to $\Sigma\Delta\varepsilon$ = 5.6 at 403 K. Changes in the average grain size evolved in the Mg alloy AZ31 during isothermal MDF at 623 K and during MDF under decreasing temperature condition are represented by a broken line and a solid line in Fig. 13, respectively (Xing et al., 2008). The average grain size developed during isothermal MDF is almost constant within the experimental scatters and about 6.7 μm at strains up to $\Sigma\Delta\varepsilon$ =4.8. On the other hand, the dynamic grain size evolved during MDF with dropping temperature condition decreases drastically with repeated MDF. Such an excellent grain refinement taking place during MDF is also observed in another Mg alloy AZ61 (Miura et al., 2008, 2010). It is concluded, therefore, that the MDF

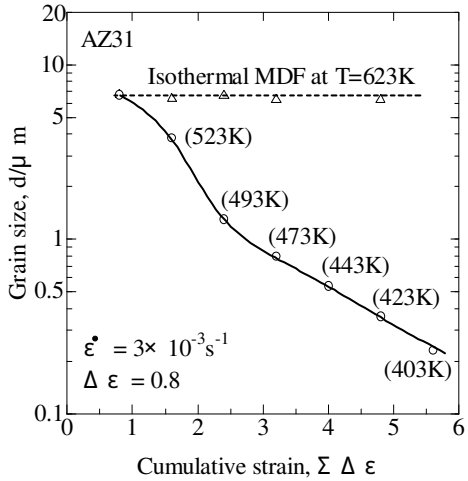

Fig. 13. Grain size changes in Mg alloy AZ31 during MDF with $\Delta\varepsilon$ = 0.8 at a temperature of 623K (broken line) or with decreasing temperature from 623K to 403K (solid line).

processing under dropping temperature conditions may be a most effective method for promotion of grain refinement in Mg alloys.

The relationship between the average grain size and the flow stress developed during MDF with dropping temperature as well as that for single-pass compression at high temperature is depicted in Fig. 14 (Xing et al., 2005, 2008). The symbols of triangle and circle indicate the data obtained by MDF and a single-pass compression at high temperature, and open and solid marks indicate the results obtained by using OM and TEM, respectively. Fig. 14 suggests that grain size may approach to 0.1 μm or less than it with further MDF at lower temperature. Such strain-induced grain sizes can be expressed by two power law functions of flow stress, i.e. $\sigma = k\, d^{-N}$, where k and N are constants, in the region of flow stress above

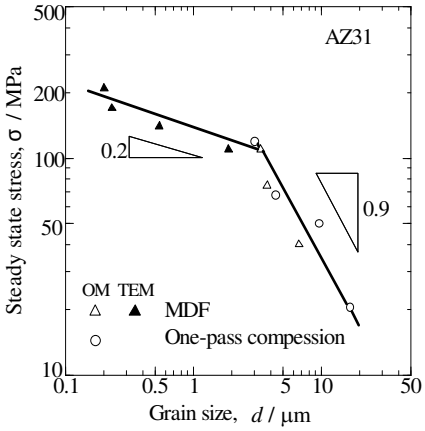

Fig. 14. Relationship between flow stress and strain-induced grain size developed during MDF and one-pass compression for Mg alloy AZ31.

or below around 100 MPa. The grain size exponent is N = 0.9 in the region of σ < 100 MPa, where deformation is carried out at higher temperatures above 0.5 T_m. In contrast, N is about 0.2 in the region of σ > 100 MPa, where MDF is performed below around 0.5 T_m. The relationship between flow stress and dynamic grain size developed in Cu and Ni-20%Cr is also roughly similar to the results in Fig. 14; namely, N is 0.75 in the region of lower stresses below 200 MPa and N = 0.3 in that of higher stresses (Belyakov et al., 2001, Dudova et al., 2010). It is interesting to note that a similar type of the relationship is held between σ and d irrespective of different recrystallization mechanisms operating in different materials, i.e. dDRX and cDRX. In pure Cu and Ni-20%Cr, dDRX and cDRX can operate in the regions of lower flow stresses and higher ones, respectively. On the other hand, only cDRX can take place in hcp Mg alloy irrespective of the flow stress regions, as discussed above.

6. Mechanical properties of fine-grained Mg alloy

Tensile specimens were machined from the Mg plate MDFed parallel to the L-ST plane, as shown in Fig. 2 (a). An UFGed structure with d = 0.36 μm was developed in this plate MDFed to $\Sigma\Delta\varepsilon$ =4.8 with decreasing temperature from 623 K to 423 K. The tensile axis is perpendicular to the final compression axis, CA (see Fig. 2(a)). Tensile tests were carried out at 298 K and at 8.3×10^{-3} s^{-1}. Fig.15 shows changes in the true stress-nominal strain (σ - ε_n) curves with strain-induced grain size at 293 K (Xing et al., 2008). The σ - ε_n curve of the 22.3 μm sample shows a monotonous work hardening following yielding and then a stress peak just before fracture at a total elongation of about 35%. It is remarkable to note in Fig. 15 that the yield and peak stresses just before fracture increase remarkably accompanying with rather large magnitude of work hardening and moderate total elongation with decreasing grain size. The σ - ε_n curve of the 0.36 μm sample shows the highest yield stress over 400 MPa and the peak stress of 526 MPa at a total elongation of 13%. This yield stress is almost 5.3 times larger than that for the as-annealed sample. Fig. 16 shows the relationships between yield flow stress at a strain of 0.2% (σ_y) or room-temperature hardness (H_v) and the average grain size (d) developed during MDF (Xing et al., 2005, 2008). The results of H_v and σ_y are represented by open and solid circles, respectively. It is noted in Fig.16 that the relationship between H_v or σ_y and d can be approximated by the following Hall-Petch equations (1) and (2) with almost similar slopes of 0.23 and 0.21.

$$H_v = 500 + 0.23\, d^{-1/2} \quad (1)$$

$$\sigma_y = 80 + 0.21\, d^{-1/2} \quad (2)$$

Here the data for the as-annealed samples are not taken into account because they do not contain deformation- induced high-density dislocations. The highest values of H_v and σ_y for the UFGed sample are over about 2 and 4 times larger than those for the annealed one, respectively. It is concluded that excellent improvement of the mechanical properties of Mg alloy can be attained by MDF processing under decreasing temperature conditions.

It is remarkable to note in Fig. 15, on the other hand, that mechanical properties of the UFGed Mg alloy are excellent for not only strength, but also ductility at ambient temperature. It has been reported in (Humphrey & Hathery, 2004, Valiev & Langdon, 2006) that such excellent mechanical properties can be attained in various UFGed materials processed by SPD. Recently, Tsuji et al. (2002) investigated the grain size dependence of room temperature strength as well as ductility of an UFGed Al alloy and an interstitial free

(IF) steel processed by the accumulative roll-bonding (ARB) method. Fig.17 shows the relationships between uniform elongation (ε_u) and strain-induced grain size (ε_u - d) for Al alloy and IF steel processed by ARB and also of the present Mg alloy processed by MDF. It can be seen in Fig.17 that grain size dependence of ε_u is almost the same in the Al and IF steel irrespective of the different crystal lattice. It is remarkable to note that the

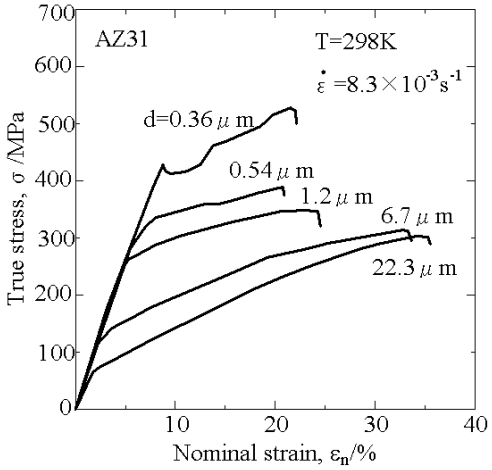

Fig. 15. Effect of strain-induced grain size on true stress-nominal strain (σ - ε_n) curves at 298K for Mg alloy AZ31 processed by MDF under dropping temperature condition.

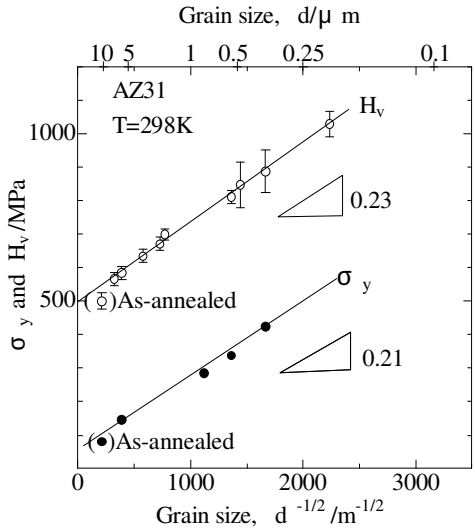

Fig. 16. Relationships between yield stress or hardness measured at 298K and strain-induced grain size developed by MDF of Mg alloy AZ31.

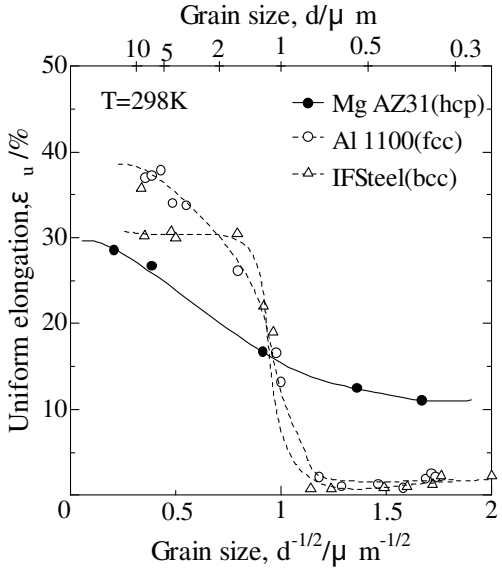

Fig. 17. Grain size dependence of uniform elongation measured in tensile tests at 298 K for Mg alloy AZ31, Al alloy 1100 and IF steel processed by severe plastic deformation. The data for Al 1100 and IF steel are reported by Tsuji et al., 2002.

uniform elongation of these metals suddenly drops to a few per cent at the grain sizes below around 1μm. In contrast, the uniform elongation of the Mg alloy does not show any drastic dropping at any grain sizes investigated and decreases gradually with decreasing grain size, and is always more than 13% even in the UFGed region. Tsuji et al. discuss that the dropping of uniform elongation taking place at grain sizes below 1 μm may be resulted from small or even negative work-hardening rate after yielding appearing in these UFGed materials, that is plastic instability.

By the way, Koike et al. (2003) studied dislocation microstructures developed by tensile deformation at room temperature for a polycrystalline Mg alloy AZ31. They observed in a 50 μm coarse-grained sample that non-basal **a** + **b** dislocations active only near grain boundaries, while basal **a** dislocations are dominant in grain interiors. In a 7 μm fine grained Mg alloy, in contrast, non-basal **a** + **b** dislocation segments are around 40% of the total dislocation density even in the grain interiors. If the data obtained by Koike et al. can be extrapolated to a range of submicron grain size, non-basal **a**+ **b** dislocations may be more activated to develop in grain interiors by compatibility stress concentration. This may activate various kinds of slip systems operating in non-basal and basal planes, and then result in relatively large work-hardening as well as moderate uniform elongation appearing in the UFGed Mg alloy, as can be seen in Fig. 17.

7. Superplasticity of fine-grained Mg alloys

Typical true stress-nominal strain (σ - ε_n) curves at various strain rates and elevated temperatures from 393K to 473K are shown in Fig. 18 (Xing et al., 2007, 2008). Strain rate

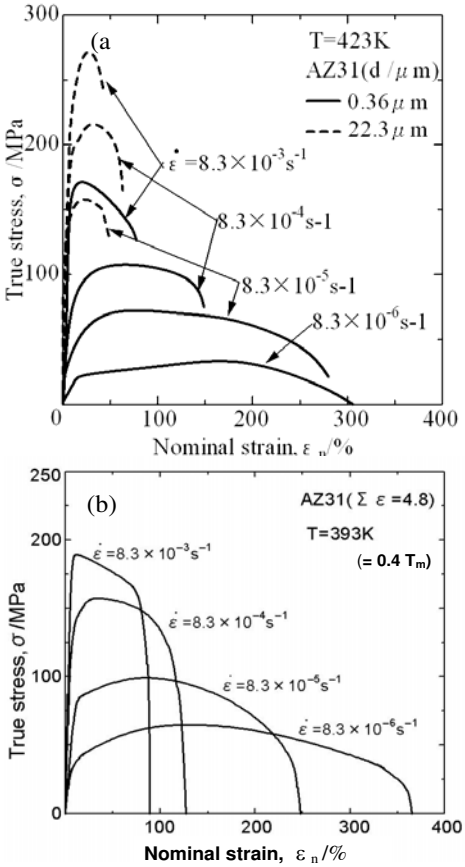

Fig. 18. (a) Effect of grain size on the strain rate dependence of true stress-nominal strain (σ - ε_n) curves at 423K and (b) strain rate dependence of σ - ε_n curves at 393 K (= 0.4 T_m) for Mg alloy AZ31 processed by MDF under dropping temperature conditions.

dependence of the flow stress peak (σ_p) and the total elongation to fracture (ε_T) are represented in Fig. 19. At the highest strain rate of around 10 $^{-2}$ s^{-1}, the σ - ε_n curves show a sharp stress peak in low strain, followed by work softening and then fracture at strains of about 100%. With decreasing strain rate, σ_p rapidly decreases and conversely ε_T increases from 100% to above 300%. At 393K and at 8.3×10 $^{-6}$s^{-1}, ε_T attains to the maximum of around 370%. A similar superplasticity was observed also in MDFed Mg alloy AZ61 (Miura et al., 2008). The superplasticity occurs at relatively low temperature (around 0.4 T_m), and so this may be defined as low temperature superplasticity. It is well known (Edington et al., 1976, Higashi et al., 1996, Nieh et al., 1997) that superplasticity can appear accompanying with a typical stress exponent ($n = \partial \ln \dot{\varepsilon} / \partial \ln \sigma$) of less than 3 and with an ε_T of above 200%. In the present experiments, however, n is always larger than 5 at strain rates investigated, while ε_T is always over 200% in strain rate below 10 $^{-3}$ s^{-1}. This result is contrast with those of general superplastic materials. This will be discussed later in detail.

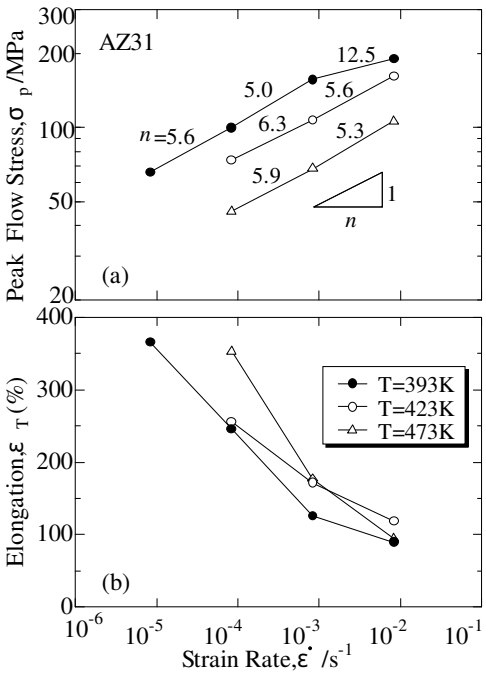

Fig. 19. Strain rate dependence of (a) peak flow stress σ_p and (b) total elongation to fracture ε_T of MDFed Mg alloy tested at 393K, 423K and 473K.

Fig. 20 shows changes in the strain-induced grain size with strain and strain rate at 473 K (Xing et al., 2007). The intial grain size of 0.36 μm in the as-MDFed samples increased to 2.2 μm during heating and keeping at 473 K before tension. It is seen in Fig. 20 that a grain structure developed by MDF is sensitively changed not only by strain rate, but also straining itself during tensile deformation. At $8.3\times10^{-5}s^{-1}$, grain size rapidly increases and attains to a peak value of 4.6 μm at $\varepsilon \cong 100\%$ and then gradually decreases to 4.1 μm at $\varepsilon \cong 350\%$. At $8.3\times10^{-4}s^{-1}$, grain size slightly increases to 2.5 μm at $\varepsilon \cong 100\%$ and then does not change in high strain. At the highest strain rate of 8.3×10^{-3} s^{-1}, in contrast, grain size decreases to 1.97 μm in early deformation and then gradually decreases with straining. At the same time, the strong texture of near {0001}; i.e. the basal plane of hcp lattice roughly parallel to the tensile axis, did not change during tensile deformation up to strain of 350% (Xing et al., 2007) (see also Fig.21). It is concluded, therefore, that the grain size of the fine-grained Mg alloy remarkably changes during superplastic deformation and, in contrast, the deformation texture is hardly changed.

Let us discuss such a characteristic superplasticity appearing in the MDFed fine-grained Mg alloy and the reason why the stress exponents are always over 3. It is generally accepted that superplasticity of fine grained materials can be controlled mainly by grain boundary sliding and so expressed by the following equation (Edington et al., 1976, Higashi et al., 1996, Nieh et al., 1997),

$$\dot{\varepsilon} = k \cdot d^{-p} \cdot \sigma^{n} \cdot \exp(-Q / RT) \tag{3}$$

where k is a constant, p is the grain size exponent, n is the stress exponent, Q is the apparent activation energy for deformation, and R is the gas constant. The n in equation (3) is obtained in the case that an initial grain size does not change during deformation. It is noted in Fig. 20 that the grain size changes depend sensitively on strain and strain rate in Mg alloy, while the changes of grain size with deformation are relatively small at high strains. The grain size developed in low strain is assumed here to be roughly constant at high strains and to depend mainly on strain rate. The relationship between the peak flow stress (σ_p) and the grain size (d) developed at around a strain associated with σ_p can be approximated by a power law function expressed by the following equation.

$$\sigma_P = k_1 \cdot d^{-N} \tag{4}$$

here k_1 and N are constants. N = 0.9 was obtained from the experimental data of Figs. 18 and 20. On the other hand, if the stress exponent is designated by n' in the present case, where d changes with deformation according to equation (4), the relationship between $\dot{\varepsilon}$ and σ_p can be approximated by equation (5).

$$\dot{\varepsilon} = k_2 \cdot \sigma_P^{n'} \tag{5}$$

It is seen in Fig. 19 that n' ranges from 5 to 6.3. Then the following relationship is derived from equations (3), (4) and (5).

$$n' = n + \frac{p}{N} \tag{6}$$

It has been reported in many superplastic metals and alloys (Edington et al., 1976, Higashi et al., 1996, Nieh et al., 1997) that p ranges from 2 to 3. If n' = 5 - 6.3 in Fig. 19, N = 0.9 and p = 2 - 3 are given in equation (6), the n takes a value of 2.8 - 3.0. This is almost similar to the

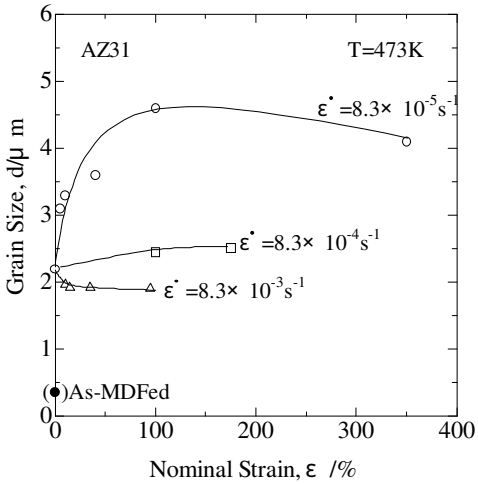

Fig. 20. Effect of strain rate on changes in average grain size with tensile deformation of MDFed Mg alloy at 473K.

typical values reported in general superplastic materials. It is concluded, therefore, that the true stress exponent of around 3 apparently increases to the experimental one of $n' = 5$ - 6.3 because the initial grain size changes sensitively with deformation.

Next let us discuss the texture change in the fine-grained Mg plate taking place during superplasticity. Fig. 21 shows OIM micrographs for a same position in the L-ST surface deformed at 473K and at 8.3×10^{-5} s^{-1} (Xing et al., 2007). It is seen in Fig. 21 that the crystal orientations of the grains marked by a, b, c and d hardly change within experimental scatters during tensile straining from $\varepsilon = 5\%$ to $\varepsilon = 40\%$. It is interesting to note that the new grains indicated by arrows in Fig.21 (b) appear in the adjoining area of the grains c and d for a strain interval between 5% and 40%. This suggests that some grains in a lower grain layer of L-ST plane may be moved to an upper layer accompanied by grain boundary sliding during deformation, that is, Fig. 21 may be an evidence for operation of the grain-switching mechanism in Mg alloy (Ashby & Verrall, 1997). It is concluded from the present study that superplasticity of fine-grained Mg alloy processed by MDF can be controlled mainly by grain boundary sliding, and at the same time grain coarsening and refinement takes place during deformation, while grain rotation hardly takes place. It is interesting to note that grain rotation hardly takes place irrespective of the operation of grain boundary sliding, and grain refinement takes place during early deformation at higher strain rate or later one at low strain rate (Fig. 20). These unusual results in Mg alloy should be investigated in more detail in the near future.

Finally let us examine the influence of the texture anisotropy of the MDFed Mg alloy on tensile deformation. Three kinds of tensile specimens, i.e. the 0°, 45° and 90°ones in Fig. 2 (b), were used for the tests. Tensile tests were performed at initial strain rates ranging from 5 $\times$ 10^{-5} s^{-1} to 5 $\times$ 10^{-3} s^{-1} and at 423 K. Typical true stress - nominal strain (σ - ε_n) curves are

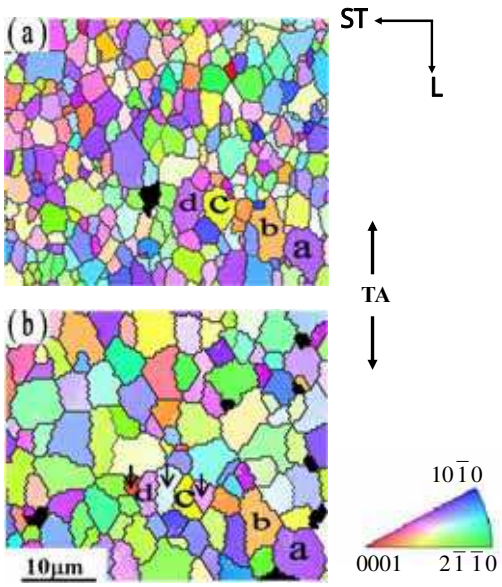

Fig. 21. OIM micrographs in L-ST surface at a same position during tensile deformation at 473 K and at 8.3 $\times$ 10^{-5} s^{-1}. (a) $\varepsilon = 5\%$ and (b) $\varepsilon = 40\%$

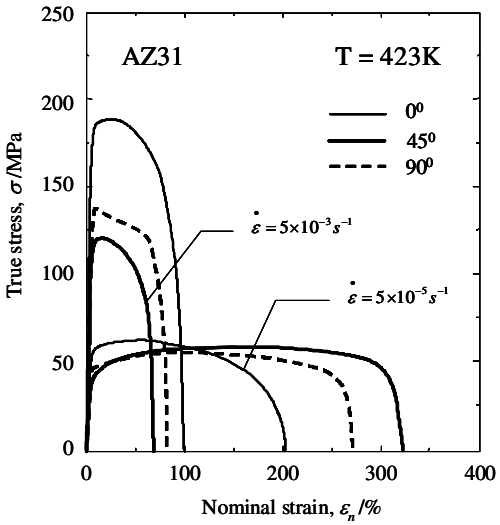

Fig. 22. True stress-nominal strain curves of MDFed Mg alloy AZ31 with different starting textures at strain rates of 5 x 10^{-5} s^{-1} and 5 x 10^{-3} s^{-1}.

represented in Fig. 22 (Zhang et al., 2009). At a higher strain rate of 5 × 10^{-3} s^{-1}, the curves show a stress peak just after yielding followed by strain softening and fracture at relatively low strain. Flow stresses decrease clearly in the order of the 0°, 90° and 45°specimen, and total elongations to failure (ε_f) of below 100% also decrease in the same order. At a lower strain rate of 5 × 10^{-5} s^{-1}, in contrast, flow curves show lower flow stresses of one-second to one-forth of those at 5 × 10^{-3} s^{-1} and large elongations to failure of over 200%. It is interesting to note that total elongations to failure increase from about 200% to 320% in the order of the 0°, 90° and 45° specimen. It is found in Fig. 22 that the mechanical properties of the present AZ31 alloy processed by MDF are sensitively affected by not only strain rate, but also the texture.

The initial texture dependence of σ_p and ε_f is depicted in Fig. 23 (Zhang et al., 2009). Anisotropy of peak flow stress resulting from the initial texture appears significantly at a higher strain rate of 5 × 10^{-3} s^{-1}. The anisotropy of σ_p decreases with decrease in strain rate and is difficult to be detected at a lower strain rate of 5 × 10^{-5} s^{-1}. However, yield stress (σ_y) at 5 × 10^{-5} s^{-1} decreases in the order of the 0°, 90° and 45° specimen, which is a similar dependence of σ_p at higher strain rates. On the other hand, texture anisotropy of ε_f also appears clearly at a strain rate of 5 × 10^{-5} s^{-1}, where all the values of ε_f are over 200%, i.e. about 320% for the 45° specimen, 280% for 90° specimen and the smallest one of 200% for 0° specimen. ε_f decreases rapidly with increase in strain rate and the anisotropy of ε_f becomes small at 5 × 10^{-3} s^{-1}.

Let us discuss such different tensile behavior appearing in the 45° or 90° specimens and in the 0° one. In the 0° specimen, slipping on basal plane and grain rotation accompanied by grain boundary sliding hardly take place during superplastic deformation, as discussed in Fig. 21. In the 45° specimen, in contrast, slip by dislocation motion additionally and easily takes place on the basal plane inclined 45° to the tensile axis and grain refinement due to cDRX may also take place in high strain during tensile deformation (see Fig. 20). This is why

larger total elongation to failure appears at 5×10^{-5} s^{-1} in the 45° or 90° specimen rather than in the 0°specimen. The various initial textures of the present alloy change with straining and approach the same stable texture in large tensile strain, i.e. the basal plane parallel to tensile axis (Zhang et al., 2009). It is concluded that superplastic deformation of the present fine-grained Mg alloy processed by MDF can be controlled mainly by not only grain boundary sliding, but also dislocation motion and grain refinement or coarsening taking place due to the operation of cDRX. The 0° specimen, in contrast, show a minimum elongation to fracture because of no texture change during tensile deformation. As a result, total elongation to failure can be affected sensitively by the initial texture of Mg specimens. However, these results should be also systematically investigated in more detail in the near future.

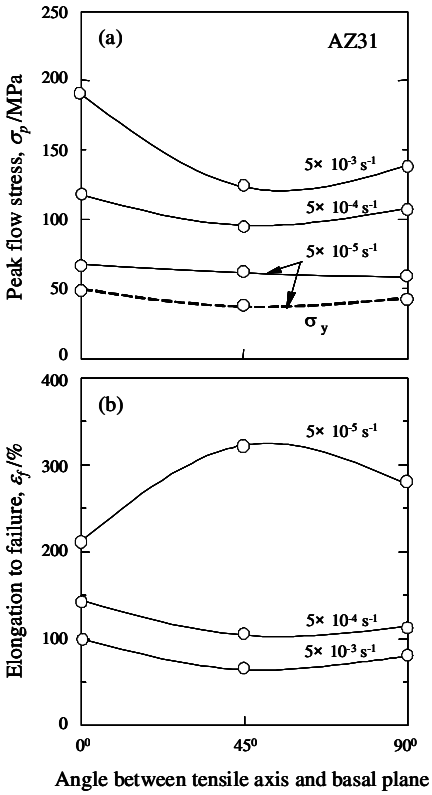

Fig. 23. Changes in (a) peak flow stress σ_p (and σ_y) and (b) elongation to failure ε_f with initial textures of MDFed AZ31 alloy tested at 423K and at various strain rates.

8. Conclusions

In magnesium (Mg) alloys categorized as hard plastic materials, fine grains are developed at relatively low strains during warm and hot working. In this chapter, optimum dynamic processes for fine grain development are studied in multi-directional forging (MDF) under decreasing temperature conditions by using commercial Mg alloys, such as AZ31, AZ61, etc.

The fine-grained Mg products processed by MDF can result in much improvement of the mechanical properties at ambient temperature and low temperature superplasticity. The main results are summarized as follows.

1. Dynamic grain evolution in Mg alloy can be resulted from grain fragmentation by kink band taking place in original grain interiors, and so controlled by deformation-induced continuous reactions assisted by dynamic recovery, i.e. continuous DRX. The grain refinement process taking place during deformation is accelerated by multi-directional forging (MDF), which is carried out with changing the loading direction from pass to pass accompanying with decrease in temperature.
2. The average grain size developed during MDF is almost constant during isothermal forging, while the one evolved under dropping temperature condition from 623 K to 403 K (< 0.5 Tm) decreases drastically with repeated MDF and approaches 0.23 μm at $\sum\Delta\varepsilon = 5.6$.
3. From the results of room temperature tensile tests for MDFed Mg alloys with a grain size of 0.36 μm, the sample shows the highest yield stress over 400 MPa and the peak flow stress of 526 MPa at a total elongation of 13%. The mechanical properties of the ultrafine grained Mg alloy are excellent for not only strength, but also ductility at ambient temperature, because various types of dislocations can be activated to operate in finer grain interiors.
4. From the results of tensile tests carrying out at temperatures from 393 K to 473 K and at various strain rates, the total elongation to fracture increases from 100 % to above 300 % and attains to the maximum of around 370 % at 393 K and at 8.3×10^{-6} s^{-1}. It is concluded that low temperature superplasticity can take place in the fine-grained Mg alloys processed by MDF. The mechanisms operated are analyzed and discussed in detail.

9. Acknowledgements

The authors are intended to Drs. Belyakov, Jonas, Kaibyshev, Sitdikov, Xing & Yang for stimulating discussions. They also acknowledge with gratitude the financial support received the following sources: the Ministry of Education, Science and Culture for some Grants-in-Aid for Scientific Research, the Japan Research Institute Advanced Copper-Base Materials and Technologies, and the Light Metals Educational Foundation, Japan, under several grants of scientific research.

10. References

Ashby, M.F. & Verrall, R.A. (1973). Diffusion-accommodated flow and superplasticity. *Acta Met.*, 21, 149-163.

Belyakov, A., Miura, H. & Sakai, T. (1998). Dynamic recrystallization under warm deformation of a 304 type stainless steel. *Mater. Sci. and Eng. A*, 255, 139 -147.

Belyakov, A., Sakai, T., Miura, H. & Kaibyshev, R. (2000). Strain-induced submicro-crystalline grains developed in austenitic stainless steel under severe warm deformation, *Philos. Mag. Letters*, 80, 711-718.

Belyakov, A., Sakai, T., Miura, H. & Tsuzaki, K. (2001). Grain refinement in copper under large strain deformation, *Philosophical Magazine A*, 81, 2629-2643.

Dudova, N., Belyakov, A., Sakai, T. & Kaibyshev, R. (2010). Dynamic recrystallization mechanisms operating in a Ni-20%Cr alloy under hot-to-warm working. *Acta Materialia*, 58, 3624-3632.

Edington, J., Melton, K.N. & Cutler, C. P. (1976). Superplasticity. *Progress in Materials Science*. 21, 61-170.

Galiyev, A., Kaibyshev, R. & Gottstein, G. (2001). Dynamic recrystallization in pure magnesium. *Acta Mater.* 49, 1199-1207.

Gao, W., Belyakov, A., Miura, H. & Sakai, T. (1999). Dynamic recrystallization of copper polycrystals with different purities, *Mater. Sci. and Eng. A,* 265, 233 - 239.

Higashi, K., Mabuchi, M. & Langdon, T.G. (1996). High-strain-rate superplasticity in metallic materials and the potential for ceramic materials. *ISIJ Intl.*, 36, 1423-1438

Higashida, K., Takamura, J. & Narita, N. (1986). The formation of deformation bands in f.c.c. crystals. *Mater. Sci. Eng.*, 81, 239-258.

Humphreys, F.J. & Hatherly, M. (2004). *Recrystallization and related annealing phenomena* (Second edition), (Elsevier, UK).

Ion, S.E., Humphreys, F.J. & White, S.H. (1982). Dynamic recrystallization and the development of microstructure during the high temperature deformation of magnesium. *Acta Metall.* 30, 1909- 1919.

Kobayashi, C., Sakai, T., Belykov, A., & Miura, H. (2007). Ultrafine grain development in copper during multidirectional forging at 195 K. *Phil. Mag. Letters,* 87, 751-766.

Koike, J., Kobayashi, T., Mukai, T., Watanabe, H., Suzuki, M., Maruyama, K. & Higashi, K., (2003). The activity of non-basal slip systems and dynamic recovery at room temperature in fine-grained AZ31B magnesium alloys. *Acta Mater.* 51 (2003), 2055-2065.

Mazurina, I., Sakai, T., Miura, H., Sitdikov, O. & Kaibyshev, R. (2008). Grain refinement in aluminum alloy 2219 during ECAP at 250 ^{o}C. *Mater. Sci. Eng. A*, 473, 297-305.

Miura, H., Aoyama, H. & Sakai, T. (1994). Grain boundary misorientation effect on dynamic recrystallization of Cu-Si bicrystals. *J. Jpn Inst. Metals*, 58, 267-275.

Miura, H., Yang, X., Sakai, T., Mogawa, R., Watanabe, T., Miura, S., & Jonas, J.J. (2005). High temperature deformation and extended elongation of Mg single crystals, *Phil. Mag.*, 85, 3553-3565.

Miura, H., Sakai, T., Mogawa, R., & Jonas, J.J. (2007). Nucleation of dynamic recrystallization and valiant selection in copper bicrystals, *Phil. Mag.*, 87, 4197-4209.

Miura, H., Yang, X. & Sakai, T. (2008). Evolution of ultra-fine grains in AZ31 and AZ61 Mg alloys during multi-directional forging and their properties, *Mater. Trans.*, 49, 1015-1020.

Miura, H, Yu, G., Yang, X. & Sakai, T. (2010). Microstructure and mechanical properties of AZ61 Mg alloy prepared by multi directional forging, *Trans. Nonferrous Metals Society of China*, 20 (in press).

Mordike, B.L. & Ebert, T. (2001). Magnesium properties - applications - potential. *Mater. Sci. Eng.* A. 302, 37-45.

Nieh, T.G., Wadsworth, J. & Sherby, O.D. (1997). *Superplasticity in metals and ceramics*, (Cambridge University Press).

Rollet, A.D. & Wright S.I. (1998). Typical textures in metals. In: *Texture and anisotropy,* Kocks, U.F., et al., (Ed.), 178-238, Cambridge University Press.

Sakai, T. & Jonas, J.J. (1984). Dynamic recrystallization: mechanical and microstructural consideration, *Acta Metalrgica.* 32, 189-209

Sakai, T. & Takahasi, C. (1991). Flow softening of 7075 aluminum alloy under hot compression, *Mater. Trans., JIM.* 32, 375-382.

Sakai, T. & Jonas, J.J. (2001). Plastic deformation: role of recovery and recrystallization, In: *Encyclopedia of Materials Science and Technology*, Buschow, K.H., et al., (Ed.), 7079-7084, (Elsevier, Oxford).

Sakai, T., Belyakov, A. & Miura, H. (2008). Ultrafine grain formation in ferritic stainless steel during severe plastic deformation, *Metall. Maters. Tra*ns. *A*, 39, 2206-2214.

Sitdikov, O. & Kaibyshev, R. (2001). Dynamic recrystallization in pure magnesium. *Mater. Trans.*, 42, 1928- 1937.

Sitdikov, O., Kaibyshev, R. & Sakai, T. (2003). Dynamic recrystallization based on twinning in coarse-grained magnesium. *Mater. Sci. Forum,* 419-422, 521- 526.

Tsuji, N., Ito, Y., Saito,Y. & Minamino, Y. (2002). Strength and ductility of ultrafine grained aluminum and iron produced by ARB and annealing. *Scripta Materialia*, 47, 893-899.

Valiev, R.Z. & Langdon, T.G. (2006). Principles of equal-channel angular pressing as a processing tool for grain refinement, *Prog. Mater. Sci.* 51, 881-981.

Wusatowska-Sarnek, A.M., Miura, H. & Sakai, T. (2002). Nucleation and microtexture development under dynamic recrystallization of copper, *Mater. Sci. and Eng. A,* 323, 177-186.

Xing, J., Soda, Y., Yang, X., Miura, H., & Sakai, T. (2005). Ultra-fine grain development in magnesium alloy AZ31 during severe large forging under decreasing temperature conditions, *Mater. Trans.,* 46, 1646-1650.

Xing, J., Yang, X., Miura, H., & Sakai, T. (2007). Superplasticity of magnesium alloy AZ31 processed by multi-directional forging, *Mater. Trans*., 48, 1406-1411.

Xing, J., Yang, X., Miura, H. & Sakai, T. (2008). Mechanical properties of magnesium alloy AZ31 after sever plastic deformation, *Mater. Trans.,* 49, 69-75.

Yang, X., Miura, H. & Sakai, T. (2002). Dynamic recrystallization and texture development in a magnesium alloy AZ31 at high temperature, *Light Metals 2002 Metaux Lergers*, Lewis, T. (Ed.), 867- 878, TMS-CIM, Montreal.

Yang, X., Miura, H. & Sakai, T. (2003). Dynamic evolution of new grains in magnesium alloy AZ31 during hot deformation, *Mater. Trans.*, 44, 197 - 203.

Yang, X., Xing, J., Miura, H. & Sakai, T. (2006). Strain-induced grain refinement of magnesium alloy AZ31 during hot forging, *Materials Science Forum,* 503-504, 521-526.

Yang, X., Miura, H. & Sakai, T. (2007). Effect of initial grain size and strain path on grain refinement in magnesium alloy AZ31, *Materials Science Forum*, 539-543, 1632-1637.

Zhang, Z.-R., Xing, J., Yang, X., Miura, H. & Sakai, T. (2009). Anisotropy of low temperature superplasticity of ultrafine grained magnesium alloy AZ31 processed by multi-directional forging, *Mater. Sci. Tech.,* 25, 1442-1447.

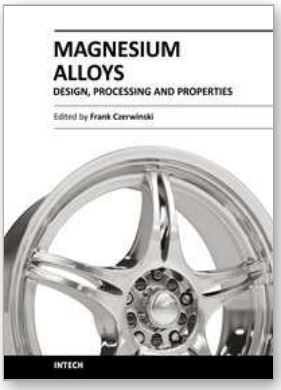

Magnesium Alloys - Design, Processing and Properties

Edited by Frank Czerwinski

ISBN 978-953-307-520-4
Hard cover, 526 pages
Publisher InTech
Published online 14, January, 2011
Published in print edition January, 2011

Scientists and engineers for decades searched to utilize magnesium, known of its low density, for light-weighting in many industrial sectors. This book provides a broad review of recent global developments in theory and practice of modern magnesium alloys. It covers fundamental aspects of alloy strengthening, recrystallization, details of microstructure and a unique role of grain refinement. The theory is linked with elements of alloy design and specific properties, including fatigue and creep resistance. Also technologies of alloy formation and processing, such as sheet rolling, semi-solid forming, welding and joining are considered. An opportunity of creation the metal matrix composite based on magnesium matrix is described along with carbon nanotubes as an effective reinforcement. A mixture of science and technology makes this book very useful for professionals from academia and industry.

How to reference

In order to correctly reference this scholarly work, feel free to copy and paste the following:

Taku Sakai and Hiromi Miura (2011). Mechanical Properties of Fine-Grained Magnesium Alloys Processed by Severe Plastic Forging, Magnesium Alloys - Design, Processing and Properties, Frank Czerwinski (Ed.), ISBN: 978-953-307-520-4, InTech, Available from: http://www.intechopen.com/books/magnesium-alloys-design-processing-and-properties/mechanical-properties-of-fine-grained-magnesium-alloys-processed-by-severe-plastic-forging

INTECH
open science | open minds

InTech Europe
University Campus STeP Ri
Slavka Krautzeka 83/A
51000 Rijeka, Croatia
Phone: +385 (51) 770 447
Fax: +385 (51) 686 166
www.intechopen.com

InTech China
Unit 405, Office Block, Hotel Equatorial Shanghai
No.65, Yan An Road (West), Shanghai, 200040, China
中国上海市延安西路65号上海国际贵都大饭店办公楼405单元
Phone: +86-21-62489820
Fax: +86-21-62489821